JOURNAL OF SOLID STATE CHEMISTRY 5, 144–152 (1972)

Energy Bands in TX_2 Compounds with Pyrite, Marcasite, and Arsenopyrite Structures*

JOHN B. GOODENOUGH

Lincoln Laboratory, Massachusetts Institute of Technology, Lexington, Massachusetts 02173

Received November 8, 1971

From symmetry arguments and the conceptual phase diagrams previously developed, it is shown that the gross features of the energy bands can be rationalized for compounds crystallizing in the pyrite, marcasite and arsenopyrite structures. The structure-determining interactions are argued to be cation–anion interactions, not cation–cation interactions. With the exception of the MnX_2 chalcogenides and $CrSb_2$, the 3d electrons appear to be itinerant, not localized; and the crystallographic determinant is not the conventional Jahn–Teller mechanism. Even the arsenopyrite structure, which would appear to reflect cation–cation homopolar bonding, may have a larger electron density in the larger cation–cation separations because the cation–anion interactions are dominant. Finally, the measured physical properties are shown to satisfy not only the requirements of the band schemes for these structures, but also the constraints of the periodic table in comparison with other transition-metal compounds.

Introduction

Hulliger and Mooser (*1*) were the first to correlate the number of transition-metal, or T-ion, *d* electrons with crystal structure in the compounds TX_2, TXY, and TY_2 having the pyrite, marcasite or arsenopyrite structures. All three of these structures are characterized by diatomic anions: formally $(X_2)^{2-}$, $(XY)^{3-}$ and $(Y_2)^{4-}$, where X is a chalcogen and Y is a pnigogen. With the assumption that the Fermi energy falls between filled anion *p* bands—with the exception of the antibonding anion-pair molecular orbitals —and empty cation *s* bands, the number of *d* electrons per cation can be obtained directly from the formal valence of the cation. Thus FeS_2 has a *d*-state manifold per iron atom d^6, FeSAs has d^5, and $FeAs_2$ has d^4. Empirically, where the d^n manifold has $n = 0$, 2, or 4, the marcasite structure is formed; where $n = 5$, either a high-spin ${}^6A_1(d^5)$ configuration in the pyrite structure or a low-spin configuration in the arsenopyrite structure is formed; and where $n \geqslant 6$, the pyrite structure is generally found, although a marcasite phase with anomalously large axial ratios may also occur. A few compounds exhibit both the anomalous marcasite and pyrite phases.

In all three structures, each anion bonds to one anion and three cations in a distorted tetrahedral coordination; and each cation has a distorted octahedral coordination of six nearest-neighbor anions. In the cubic pyrite structure, the ions form the face-centered-cubic array of the rocksalt structure, and the axes of the diatomic anions are ordered equally along the four <111> directions of the cube, as shown in Fig. 1. The cation octahedra share common corners, and the resulting crystal field at a transition-metal ion has trigonal symmetry. In the orthorhombic marcasite structure of Fig. 2, on the other hand, linear chains of edge-shared octahedra run parallel to the orthorhombic *c*-axis. Two forms of marcasite have been distinguished: regular marcasite having a cation–anion–cation angle $\alpha < 90°$ along the *c*-axis, and anomalous marcasite having an $\alpha > 90°$. The latter form is found in compounds having $n \geqslant 6$, the former in those having $n \leqslant 4$. Finally, the monoclinic arsenopyrite structure is a distorted marcasite in which the chains of cations parallel to the *c*-axis form alternately short and long separations,

* This work was sponsored by the Department of the Air Force.

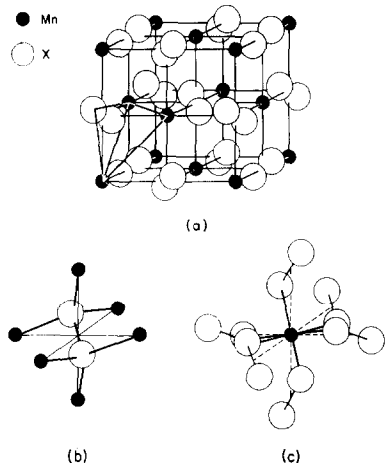

FIG. 1. The pyrite structure.

which has suggested (*1*) T–T homopolar-bond formation along the *c*-axis.

Hulliger and Mooser pointed out that the one-electron *d* orbitals would be split by the crystalline fields as indicated schematically in Fig. 3. With the assumption that these splittings are large compared to any bandwidths, they showed that the magnetic and electrical properties of these compounds may be satisfactorily accounted for if the d_{xy} orbital, which is directed toward near-neighbor cations along the *c*-axis,

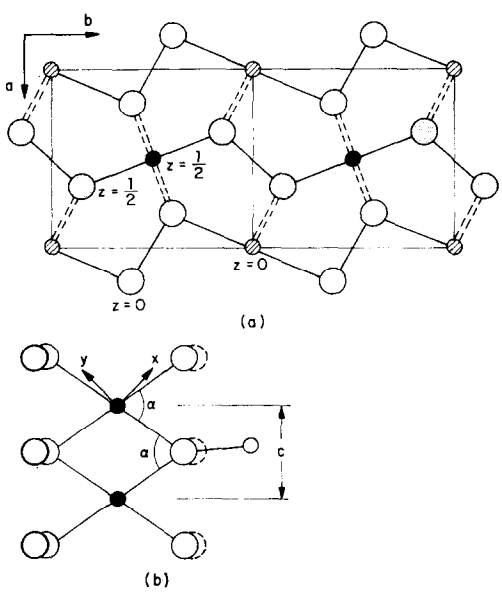

FIG. 2. The orthorhombic marcasite structure: (*a*) projection onto *a*–*b* plane, (*b*) a *c*-axis chain in the regular marcasite structure.

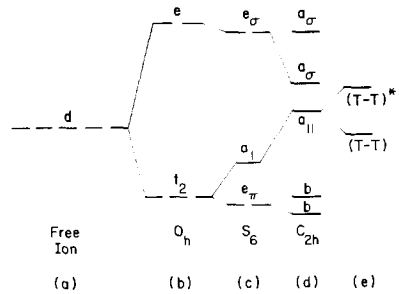

FIG. 3. Hulliger–Mooser one-electron *d*-level scheme per cation: free atom (*a*) and octahedral-site splittings in (*b*) cubic, (*c*) pyrite, (*d*) marcasite and (*e*) arsenopyrite crystalline fields.

is less stable than the d_{yz} and d_{zx} orbitals—provided the d^2 and d^5 manifolds at Cr^{4+} and Mn^{2+} ions are split into α-spin and β-spin states by intraatomic exchange forces so as to give atomic moments $\mu_{Cr} \approx 2\mu_B$ and $\mu_{Mn} \approx 5\mu_B$. Given a local octahedral-site symmetry C_{2h} and the coordinate axes of Fig. 2, the $a_{\parallel}$ orbital of Fig. 3 is primarily associated with d_{xy} and the two *b* orbitals with d_{yz} and d_{zx}. The more stable of the two a_σ orbitals is primarily associated with the $d_{x^2-y^2}$ orbital, the less stable with the d_{z^2} orbital.

The model proposed by Hulliger and Mooser contains four principal defects: (1) The authors assumed that the *d* electrons are sufficiently localized that single-atom Jahn–Teller deformations occur, and that these deformations are responsible for stabilization of the alternate structures. (2) The authors assumed that, although the electrons are localized, nevertheless in the $d_{\parallel}$ configuration crystal-field splittings of the $a_{\parallel}$ orbital from the two *b* orbitals must be larger than any intraatomic exchange splitting Δ_{ex}, since these compounds exhibit no spontaneous magnetization. No justification for this assumption was, or can be, offered. (3) Formation of the arsenopyrite structure for compounds with the d^5 configurations was assumed, without supporting arguments, to be due to T–T homopolar bonding. (4) No indication was given that the formal-valence concept might break down and under what conditions it would no longer be meaningful.

Subsequently Brostigen and Kjekshus (*2*) reexamined the geometrical relationships between the pyrite and marcasite structures and observed that the smaller axial ratios *c*/*a* and *c*/*b* of the regular marcasites, which occur where $n \leqslant 4$, can be nicely accounted for by a simple reorientation

of the axes of the diatomic anions from their directions in the pyrite structure. Therefore, they argued that it is not necessary to introduce a Jahn–Teller mechanism to stabilize the regular marcasite structure, as proposed by Hulliger and Mooser, and that the small axial ratios c/a and c/b of regular marcasite do not reflect c-axis compressive forces due to metal–metal bonding, as proposed by Pearson (*3*). Instead, they proposed an "expansion model" in which the larger axial ratios of anomalous marcasite are due to expanding forces along the c-axis. Further support for eliminating a conventional Jahn–Teller mechanism for stabilizing the regular marcasite structure came from their observation (*4*) that the marcasite forms of FeS_2, $FeTe_2$ and $CoTe_2$ all have the space group P*nn*2 rather than the more symmetric space group P*nnm* generally assumed. In order to rationalize their expansion model, Brostigen and Kjekshus (*5*) then argued that the $a_{\parallel}$ orbital is destabilized relative to the two b orbitals by coulomb repulsive forces between the electrons in neighboring $a_{\parallel}$ orbitals.

Despite an apparent two-parameter fit of the variation in c/a and c/b with electron–atom ratio, the proposed expansion model contains a fatal defect. Within a cation subarray, any cation–cation interactions between electrons in orbitals that are half-filled or less are bonding and, therefore, attractive. On the basis of cation–cation interactions it is necessary to attribute formation of the arsenopyrite structure to T–T homopolar bonding, as proposed by Hulliger and Mooser and by Pearson. Furthermore, the idea that π bonding with the anions plays a role in the repulsive mechanism was explicitly rejected (*6*), even though the fact that the d orbitals are antibonding with respect to the anion array would make the cation–anion interactions a logical source of repulsive force for expanding the c-axis with $a_{\parallel}$-orbital occupancy, as I shall point out below.

The purpose of this paper is to argue for a more realistic physical basis for the empirical regularities first pointed out by Hulliger and Mooser.

General Considerations

Construction of an energy-band scheme begins with the energy difference E_M-E_I between cation s and anion p outer orbitals for an ionic structure, where E_M is the Madelung energy for the effective ionic charges and E_I includes the anion affinity as well as the cation polarization energy. Outer s and p orbitals are primarily responsible for the binding energy of a crystal, and they interact strongly with the neighboring atoms. Therefore, they generally form bands of itinerant-electron energies. Itinerant cation and anion orbitals having the same symmetry properties interact with one another producing covalent mixing. This mixing stabilizes the anion states, which are bonding with respect to cation–anion interactions, and destabilizes the cation states, which are antibonding with respect to these interactions. Compounds tend to crystallize into structures that permit all the anionic bonding states to be occupied and all the antibonding states to be empty. Nonbonding (with respect to the sublattice of opposite character) orbitals may be occupied—this is the basis of the empirical (8-N) rule—or empty. In some compounds, stabilization of any structure having single-atom anions would leave the Fermi energy E_F below the top of the bonding, anion p bands. In these cases, nature forms multiatom anions. The three structures: pyrite, marcasite, and arsenopyrite, are characterized by diatomic anions. These signal the formation of a single anion-pair bond, which means that the interacting orbitals per anion pair are split into a filled, bonding molecular σ_M orbital and an empty, antibonding molecular $\sigma_M{}^*$ orbital. If the hypothetical structure having single-atom anions were to contain one (or less) holes per anion in the anion p bands, then formation of diatomic anions would lift the Fermi energy above the top of the anion p bands.

Transition-metal compounds contain outer d orbitals. So long as the Fermi energy falls in the energy gap between occupied, anion p orbitals and empty cation s and any $\sigma_M{}^*$ orbitals, then assignment of a formal valence to the cation indicates the number of d electrons per cation. Furthermore, if the d electrons are localized, then successive multielectron energies for the d^n manifold are separated by finite energies, as illustrated in Fig. 4 for MnS_2. On the free atom, these successive energies may be estimated from the successive ionization potentials. Where the d-state manifold is close to the atomic s and p energies, as occurs in lighter transition elements of any long period, hybridization between cation d, s and p states tends to extend the "d" wave functions, thereby lowering the electrostatic energy $U = E_{n+1} - E_n$ separating the d^n from the d^{n+1} manifold. In a crystal, the ionic "d" wave

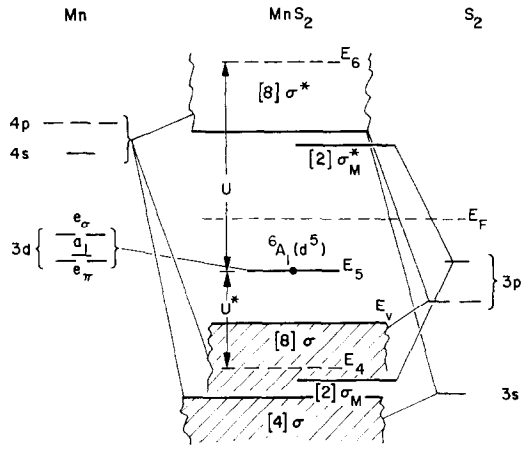

FIG. 4. Energy-level scheme for MnS_2. One-electron energies for s and p bands, energy E_5 of ${}^6A_1(d^5)$ single-atom manifolds and energies E_6 and E_4 of the d^6 and d^4 single-atom manifolds. Numbers in brackets refer to states per molecule.

functions are replaced by crystal-field wave functions

$$\psi_\Gamma = N(f_\Gamma - \lambda\phi_\Gamma) \tag{1}$$

where N is a normalization constant, f_Γ is the ionic orbital having symmetry representation Γ, and λ is the covalent-mixing parameter for the symmetrized anion wave function ϕ_Γ:

$$\lambda \sim b_\Gamma^{\mathrm{ca}}/(E_{n+1} - E_p). \tag{2}$$

Here b_Γ^{ca} is an anion-to-cation transfer integral:

$$b_\Gamma^{\mathrm{ca}} = (\psi_\Gamma, \mathscr{H}'\phi_\Gamma) \sim \epsilon(\psi_\Gamma, \phi_\Gamma) \tag{3}$$

in which $\mathscr{H}'$ represents the perturbation of the ionic potential at the anion array by the presence of the d^n cations, and E_p is the energy of the anion p orbitals. For any given atom, the energy difference $(E_{n+1} - E_p)$ increases with n, and below a critical value of n for the heavier transition elements of any long period the Fermi energy would fall below the top of the anion p bands. This limits the magnitude of the formal valences that can be stabilized. Furthermore, as n decreases for a given T atom, the parameter λ increases to extend the crystal-field wave functions ψ_Γ out over the anions. Thus in a crystal the energy U between d-state manifolds tends to be a maximum if the energy E_n is well below the cation s band and the energy E_{n+1} is well above the top of the anion p band. This situation is optimized for the high-spin d^5 configuration of MnS_2, since intraatomic exchange stabilizes this configuration relative to the d^6 configuration. (The sixth d electron is screened from the atomic nucleus by all the other five d electrons, whereas in the high-spin d^5 configuration each electron occupies a different d orbital and is therefore only partially screened by the other outer electrons.) Finally, any bandwidth due to interactions between crystal-field d orbitals is (7)

$$W \approx 2zb \tag{4}$$

where z is the number of near neighbors and

$$b = (\psi_i, \mathscr{H}\psi_j) \approx \epsilon_{ij}(\psi_i, \psi_j) \tag{5}$$

is the one-electron transfer integral for overlapping orbitals at the near-neighbor positions $\mathbf{R}_i$ and $\mathbf{R}_j$. The condition for localized d electrons is

$$W \ll U, \tag{6}$$

and the condition for itinerant d electrons with only weak correlation is

$$W \gg U. \tag{7}$$

Itinerant d electrons having correlations strong enough to introduce spontaneous magnetism and to split half-filled bands in two are found where

$$W \approx U. \tag{8}$$

It follows that the most probable localized-electron configuration is d^5 at a cation of relatively low formal valence state: i.e., Mn^{2+}. Whereas lighter transition-metal cations of low formal valence may have cation-hybridized "d" wave functions of sufficient radial extension to create itinerant "cation–sublattice" d bands, heavier cations and those of higher formal valence may have a sufficiently large λ, and hence large $W \sim \epsilon\lambda^2$ and small U, to create itinerant "total-lattice" d bands. Furthermore, the more polarizable the anion, the larger is any b^{ca}, and hence any λ. Therefore localized $3d$ electrons are more common in transition-metal oxides than in sulfides, in sulfides than in selenides; or in fluorides than in oxides, in oxides than in phosphides.

The electrostatic energy U decreases with increasing radial extension of the crystal-field wave functions of Eq. (1), and hence with increasing λ for the heavier transition elements. (Decreasing dsp hybridization on the cation reduces the radial extension of f with increasing

atomic number, and this appears to be more important for the lighter transition elements.) Furthermore, from Eqs. (4) and (5) any bandwidth due to T–X–T interactions increases as

$$W \sim 2z\epsilon_{ij}N^2\lambda^2. \quad (9)$$

It follows that for the heavier elements in any long period the ratio W/U increases unambiguously with the covalent-mixing parameter λ. Therefore any interpretation of the physical properties of the compounds TX_2, TXY or TY_2 must be consistent with this prediction. In addition, from the physical properties of several transition-metal sulfides, there appears to be a transition from localized σ-bonding d electrons at Mn^{2+} ions to itinerant, but usually strongly correlated σ-bonding d electrons at Ni^{2+} ions (*8*). In some structures the Fe^{2+} and Co^{2+} ions are stabilized in a high-spin state with localized σ-bonding d electrons; in others they are stabilized in a low-spin state with itinerant σ-bonding d electrons.

With this general orientation, we are now in a position to construct the essential features of the band schemes necessary for interpreting the physical properties of the TX_2 compounds having pyrite, marcasite or arsenopyrite structures.

Band Schemes

The Pyrites

In the pyrite structure each anion has one anion and three cation near neighbors at the corners of a distorted tetrahedron (bond angles $109 \pm 7°$ in FeS_2); the cations occupy a distorted octahedral interstice (having bond angles $90 \pm 5°$ in FeS_2). Thus each anion forms four covalent

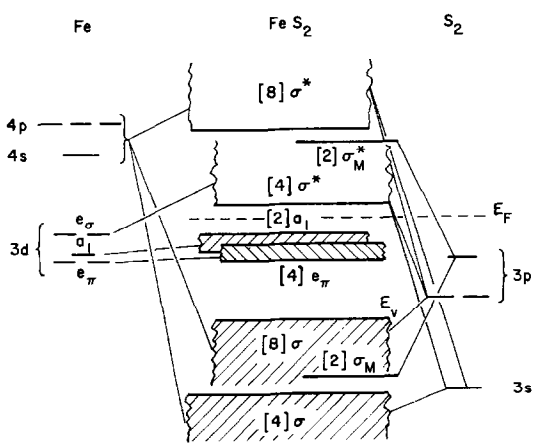

FIG. 5. Energy bands for FeS_2 with the pyrite structure.

(sp^3) bonds, one of which creates an antibonding, molecular σ_M* orbital that is empty and three of which σ-bond with the six σ-bonding orbitals $e_\sigma^2 sp^3$ per cation. Of the orbitals involved in bonding between the cation and anion sublattices, the primarily anionic orbitals are bonding and, therefore, stabilized by the covalent mixing whereas the primarily cationic orbitals are antibonding and destabilized as indicated in Fig. 5. With the exception of the MnX_2 chalcogenides, which contain a localized-electron manifold $^6A_1$ (high-spin d^5) similar to that found in the MnX monochalcogenides, covalent mixing with the two σ-bonding d orbitals of e symmetry (designated e_σ) is sufficiently strong to create a narrow σ* band of itinerant-electron states and to put the cation in a low-spin state, where any intraatomic exchange splitting Δ_{ex} is less than the crystal-field splitting parameter

$$10\ \mathrm{Dq} \sim (\lambda_\sigma^2 - \lambda_\pi^2)(E_{n+1} - E_p) \quad (10)$$

Therefore the diamagnetic semiconductor FeS_2 has a band structure like that shown in Fig. 5, whereas the antiferromagnetic chalcogenides MnX_2 have an energy band scheme described by Fig. 4. The energy of the $^6A_1$ manifold may drop below E_v, the top of the anion p bands, in $MnTe_2$, and perhaps even in $MnSe_2$. In Fig. 5 the narrow, primarily nonbonding e_π and a_1 bands are shown split in order to emphasize the existence of a trigonal component to the crystalline fields at a T atom. Any hole mobility in FeS_2 should be smaller than the electron mobility, and an activated hole mobility would signal small-polaron formation in the narrow a_1 bands.

Correlation of the physical properties of the pyrites FeX_2, CoX_2, NiX_2 and CuX_2 with the band model of Fig. 5 has been discussed elsewhere (*9*). For a given chalcogenide anion X, the narrow σ* bands contain more electrons and drop relative to E_v with increasing atomic number of the T atom. In the superconductor CuS_2 it is not possible to predict unambiguously from these simple considerations whether, as shown in Fig. 6, E_v overlaps the σ* bands sufficiently to create holes in the anion p bands, thereby rendering meaningless any formal valence at the copper atoms. From the peculiar structure of covelline, CuS, it would appear that holes are present in both the copper d bands and the anion p bands in the sulfides. However, in the other compounds of this series, with the possible exception of the nonstoichiometric tellurides, a formal valence

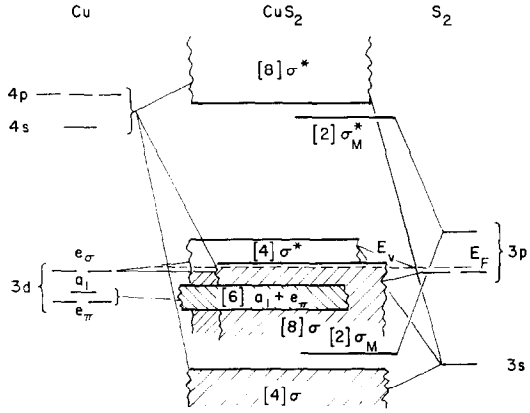

FIG. 6. Probable energy-band scheme for CuS_2.

is meaningful. Therefore the change from ferromagnetism in metallic CoS_2 to antiferromagnetism in metallic $CoSe_2$ could be attributed (*9*) to a quarter-filled σ^* band having electron correlations that are just strong enough to sustain spontaneous magnetism (as a spin-density wave) in $CoSe_2$. Although these correlations are stronger in CoS_2, they are still not strong enough to produce a full atomic moment of $1\mu_B$/low-spin Co^{2+} ion. From the saturation magnetization of CoS_2 *a* $\mu_{Co} \approx 0.9\mu_B$ is obtained. Similarly, the change from an antiferromagnetic semiconductor in NiS_2 to a paramagnetic metal in $NiSe_2$ was attributed to a half-filled σ^* band having electron correlations just strong enough to sustain spontaneous magnetism in the sulfide. The electron correlations also split the half-filled σ^* band in two. This interpretation is quite consistent with the observation of a first-order semimetal-to-metal transition in NiS at a Néel temperature. The somewhat larger λ_σ in NiX_2 than in CoX_2 is predicted from Eq. (2), since nickel is to the right of cobalt in the periodic table.

In conclusion, compounds crystallizing in the pyrite structure have either filled e_π and a_1 orbitals, or half-filled e_π and a_1 orbitals that are localized. In addition, they exemplify localized 3d electrons in the antiferromagnetic semiconductors MnX_2 having $\mu_{Mn} \approx 5\mu_B$, itinerant 3d electrons with weak electron correlations in the superconductor CuX_2, and itinerant 3d electrons with strong correlations in the compounds CoX_2 and NiX_2, three of which exhibit spontaneous magnetism.

The Marcasites

The essential difference between the band structure of the pyrites and that of the marcasites and arsenopyrites is the splitting of the t_{2g} orbitals, as was first pointed out by Hulliger and Mooser (*1*) (see Fig. 3). The three S–S–Fe angles in marcasite FeS_2 are 103.3, 107.2 and 107.5°, the As–As–Fe angles in $FeAs_2$ are one at 111.8° and two at 107°, and the Sb–Sb–Fe angles in $FeSb_2$ are 105.3, 107.2, and 107.5° (*4, 10*). These are all close to the ideal tetrahedral angle, which means that with reference to the anion-pair bond direction all the cations nearest-neighbor to an anion are located essentially on the cone surface generated by rotation of a tetrahedral-bond angle about the anion-pair bond axis. However, within that cone surface the Fe–X–Fe bond angles are distorted from the tetrahedral angle by having a small Fe–X–Fe angle α associated with the shared octahedral-site edges along the *c*-axis (see Fig. 2). Similarly the X–Fe–X angles of an octahedral site are $90 \pm 3°$ if one Fe–X direction is parallel to the *z*-axis, whereas within the *x–y* plane (coordinates as shown in Fig. 2) the angle α is only 72.5° in $FeAs_2$ and 76° in $FeSb_2$, but 97.5° in the marcasite form of FeS_2. From these geometrical considerations, it is clear that the $a_\parallel$ orbital is not orthogonal to the σ-bonding anion orbitals, whereas the two *b* orbitals are nearly so. Therefore, the $a_\parallel$ orbital is distinguished from the two *b* orbitals by relatively strong covalent mixing with the anion orbitals, and the strength of this mixing increases with the deviation of α from 109°. Since the *d* orbitals are only antibonding with respect to the anion array (they are bonding and antibonding with respect to the cation array), they are destabilized by covalent mixing. Therefore the $a_\parallel$ orbital is destabilized relative to the two *b* orbitals, as was first conjectured by Hulliger and Mooser to account for the empirical correlation between structure, physical properties, and electron-atom ratio. The fact that $FeAs_2$ is a diamagnetic semiconductor requires that in $FeAs_2$ this destabilization be strong enough to raise the $a_\parallel$ band completely above any narrow *b* bands, as shown in Fig. 7. Furthermore, in order for the splitting between the $a_\parallel$ and two *b* orbitals to be large enough to quench any spontaneous magnetism, it appears necessary to have sufficient covalent mixing to create an $a_\parallel$ band of itinerant-electron states.

Since covalent mixing stabilizes bonding, primarily anionic states at the expense of antibonding, primarily cationic states, stronger covalent mixing occurs with empty cationic orbitals. (Half-filled *d* orbitals containing localized electrons of

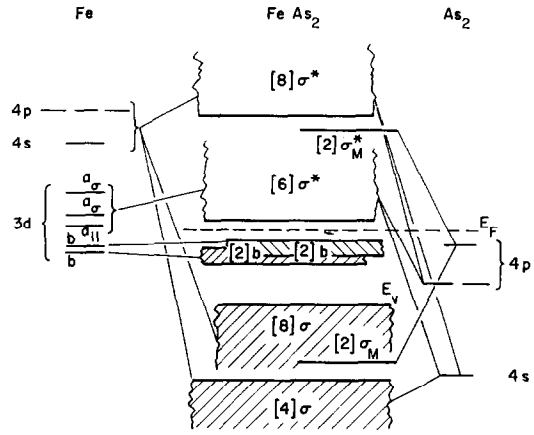

FIG. 7. Energy bands for $FeAs_2$ with the regular marcasite structure.

α spin may have relatively strong covalent mixing with empty β-spin orbitals.) Furthermore, structures that optimize covalent bonding are generally favored. Therefore an octahedral-site coordination is favored for cations having a localized d^3 or d^8 configuration or a nonmagnetic d^6 configuration: $t_{2,\alpha}^3e^0$, $t_2{}^6e_\alpha{}^2$, and $t_2{}^6e^0$. Similarly a tetrahedral-site configuration may be stabilized by a stable (not too strong dsp hybridization) d^0 configuration, a localized d^2 or d^7 configuration, or a nonmagnetic d^4 configuration: $e^0t_2{}^0$, $e_\alpha{}^2t_2{}^0$, $e^4t_{2,\alpha}^3$, and $e^4t_2{}^0$. The orthorhombic configuration of the marcasite structure, like the tetrahedral-site coordination of cubic symmetry, allows σ-bond covalent mixing with three of the five d orbitals: the two a_σ and $a_\parallel$, and bonding with the $a_\parallel$ orbital is larger the smaller the angle α. Therefore regular marcasite should be the competitive TX_2 structure for T cations having a d^0 configuration, a localized d^2 or d^7 configuration or a nonmagnetic d^4 configuration: $b^0a_\parallel{}^0a_\sigma{}^0$, $b_\alpha{}^2a_\parallel{}^0a_\sigma{}^0$, $b^4a_{\parallel,\alpha}^1$, $a_{\sigma,\alpha}^2$, and $b^4a_\parallel{}^0a_\sigma{}^0$. Note that the relatively small axial ratios c/a and c/b of the regular marcasite structure are due to cation-anion bonding, not to cation-cation bonding. Compounds crystallizing in the regular marcasite structure include: $Mo_{2/3}\square_{1/3}As_2(d^0)$, antiferromagnetic ($\mu_{Cr} \approx 2\mu_B$ and $T_N = 273°K$ [11]) $CrSb_2(d^2)$, and the $TY_2(d^4)$ compounds having T = Fe, Ru, or Os and Y = P, As, or Sb. The $CoX_2(d^7)$ chalcogenides contain itinerant d electrons, which stabilizes the Co^{2+} ions in the pyrite structure with the low-spin $a_1{}^2e_\Pi{}^4\sigma^{*1}$ state. Superconducting $AuSb_2$, which also has the pyrite structure, not only contains itinerant d electrons, but also can be expected to have holes in the anion p bands as well as in the narrow σ^* bands. Assignment of formal valences with a corresponding d^7 configuration on the gold atoms is undoubtedly quite misleading.

It is interesting that no T ions having d^1 or d^3 configurations have been reported to crystallize in the pyrite or marcasite structures. Localized d^3 configurations are generally found at Cr^{3+} ions in sulfides, and it would be interesting to know whether a magnetic CrSAs can be stabilized with the pyrite structure. A d^1 configuration or an itinerant-electron d^3 configuration should stabilize the marcasite structure in preference to the pyrite structure. However, TX_2 compounds that would stabilize a d^3 configuration in the marcasite structure generally have sufficiently unstable d electrons that they crystallize in layer structures with stable d^1 configuration. (The layer compounds have single-atom anions.)

If the d^n configuration at a T atom has $n > 4$, then crystallization in the marcasite structure leaves antibonding electrons in the $a_\parallel$ orbitals. Antibonding $a_\parallel$ electrons introduce a c-axis repulsive force between the cations and the anions that increases the angle α, thereby stabilizing the $a_\parallel$ band and destabilizing one of the a_σ bands. It follows that the $a_\parallel$ band splits away from the a_σ bands and approaches the two b bands with increasing angle α. Therefore in the marcasite form of FeS_2, which has $n = 6$, the structure has an anomalously large angle $\alpha = 97.5°$ in contrast to $\alpha = 72.5°$ in the regular marcasite $FeAs_2$. Clearly the angle α, and hence the axial ratios c/a and c/b, must increase monotonically with the number of $a_\parallel$ electrons from a constant value for $n \leqslant 4$ to a larger constant value for $n \geqslant 6$, in conformity with the finding of Brostigen and Kjekshus (*5*). However, the origin of the expansion forces is seen to be a cation–anion interaction, not a cation–cation interaction. Furthermore I have argued that stabilization of the regular marcasite structure relative to the pyrite structure is due to enhanced cation–anion d-orbital bonding. By the same argument, loss of this enhanced bonding would make the energies of the anomalous–marcasite and pyrite structures comparable, which is compatible with the existence of both phases in FeS_2 and $CoSe_2$.

The fact that $FeAs_2$ is a semiconductor at room temperature, whereas $FeSb_2$ may be a semimetal (*12*), is compatible with the larger α in $FeSb_2$, since the relative stability of the $a_\parallel$ band increases

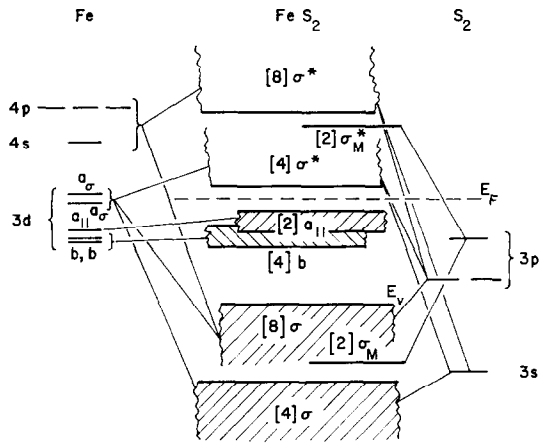

FIG. 8. Energy bands for FeS_2 with the anomalous marcasite structure.

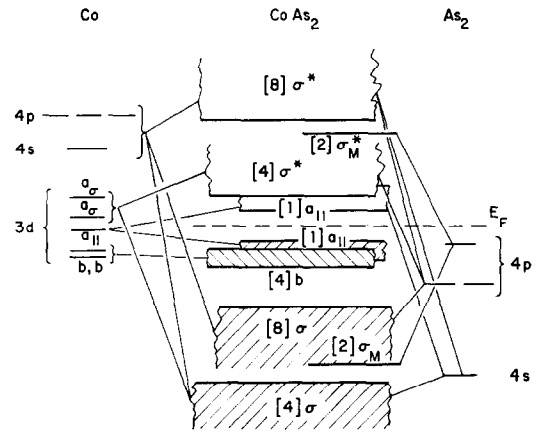

FIG. 9. Energy bands for $CoAs_2$ having the arsenopyrite structure.

with α. This finding indicates that the $a_{\parallel}$ and the two b bands all overlap in the anomalous marcasites, as indicated in Fig. 8 for semiconducting FeS_2 with the marcasite structure.

The Arsenopyrites

The fact that the arsenopyrite structure is uniquely associated with compounds having a low-spin d^5 configuration also follows from these considerations. Given the band scheme of Fig. 7 for a T ion with d^4 configuration, such as $FeAs_2$, it follows that $CoAs_2$ would have a half-filled $a_{\parallel}$ band if it crystallized in the marcasite structure. It is now well recognized (*7*) that a narrow, half-filled d band may induce a crystallographic distortion that changes the structural periodicity so as to split the band in two, thereby stabilizing occupied bonding states and destabilizing only empty antibonding states. Therefore the distortion from the marcasite to the arsenopyrite structure is most reasonably interpreted to reflect a similar instability, especially in view of the double periodicity along the c-axis. It follows at once that the band structure for the arsenopyrite structures would be similar to those for the marcasite structures, but with a splitting of the narrow $a_{\parallel}$ band as shown in Fig. 9; and that these structures should be diamagnetic semiconductors, as is known experimentally. Furthermore, the possibility exists that at higher temperatures and/or pressures some of these compounds may exhibit semiconductor-to-metal transitions associated with a first-order phase change from the arsenopyrite to the marcasite structure.

The band structure of Fig. 9 still begs the question of the electron-density distribution due to the d_{xy} electrons. The compound VO_2 exhibits an apparently analogous cation–cation pairing along the c-axis of the rutile structure below a nonmagnetic semiconductor-to-metal transition at $T_t \approx 70°C$. In this compound sufficiently strong metal-metal interactions cause localization of the single d electron per V^{4+} ion in homopolar V–V bonds. Antiferroelectric displacements of the cations perpendicular to the c-axis simultaneously optimize bonding between filled anion–$2p_{\pi}$ orbitals and empty cation-3d orbitals (*13*). In the arsenopyrites the situation, though analogous, is somewhat different. Here the cation–anion interactions appear to play a more dominant role than any cation–cation interactions, so that the distortion may not consist so much of T–T pairing along the c axis as an opening of alternate angles α along the c axis. Opening of the T–Y–T bond angles reduces covalent mixing, thereby stabilizing the antibonding orbitals, and an alternation of smaller and larger angles α should concentrate the $a_{\parallel}$-electron density between the expanded links of the c-axis chain of cations. Formation of homopolar T–T bonds would concentrate the charge density in the shorter links. Thus rather than a distortion that reflects T–T homopolar bonding, the arsenopyrite structure may exemplify a distortion due to cation–anion repulsive forces along the c axis. This description is compatible with the crystallographic alterations emphasized by Brostigen and Kjekshus (*5*), but attributes the repulsive forces to cation–anion interactions rather than to cation–cation interactions. Any cation–cation interactions would be attractive, as is observed in VO_2.

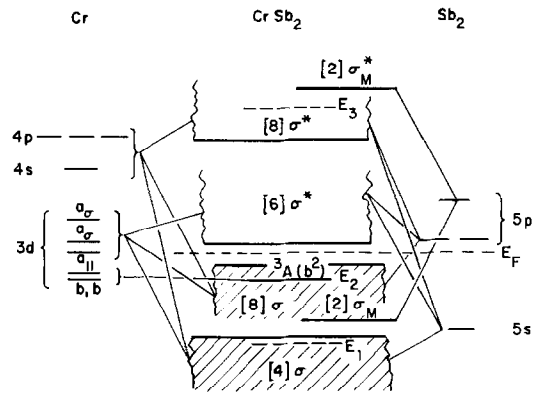

FIG. 10. Energy-level scheme for antiferromagnetic $CrSb_2$. One-electron energies except for the ^3A single-atom manifold associated with localized d electrons in the two b orbitals of α spin.

Conclusions

From comparisons of the physical properties of the known TX_2, TXY, and TY_2 compounds, it is possible to draw the following conclusions:

1. The empirical energy splittings used by Hulliger and Mooser (*1*) to correlate physical properties with electron–atom ratio are essentially correct, but the d electrons are probably only localized in the antiferromagnetic compounds $CrSb_2$ and MnX_2. In addition, splitting of the $a_{\parallel}$ band in the arsenopyrite structure may not be due to the formation of T–T homopolar bonds, and the superconductivity of the CuX_2 pyrites as well as the nonstoichiometry of $FeTe_2$ and $CoTe_2$ may be due to overlapping of the anion p bands and cation σ^* bands that renders formal valences meaningless.

2. Although the expansion model of Brostigen and Kjekshus (*5*) has some attractive features, the physical origin of the repulsive forces along the c axis of the marcasite structure for $n > 4$ is the cation–anion interaction associated with antibonding $a_{\parallel}$ electrons and not a cation–cation interaction.

3. The appearance of itinerant *vs.* localized $3d$ electrons and of spontaneous itinerant-electron magnetism is consistent with the conceptual phase diagrams previously developed (*7, 9*) and with the known occurrences of localized electrons and spontaneous itinerant-electron magnetism in other transition-metal compounds.

4. Antiferromagnetic $CrSb_2$ probably contains both localized and itinerant d orbitals, as indicated in Fig. 10, the two d electrons per Cr^{4+} ion occupying a localized ^3A state.

5. A compound having localized d^3 configuration, such as hypothetical CrSAs, is predicted to be more stable in the pyrite or anomalous marcasite structure than in the regular marcasite structure.

References

1. F. HULLIGER AND E. MOOSER, *J. Phys. Chem. Solids* **26**, 429 (1965).
2. G. BROSTIGEN AND A. KJEKSHUS, *Acta Chem. Scand.* **24**, 2983 (1970).
3. W. B. PEARSON, *Z. Kristallogr. Kristallgeometrie, Kristallphys, Kristallchem.* **121**, 449 (1965).
4. G. BROSTIGEN AND A. KJEKSHUS, *Acta Chem. Scand.* **24**, 1925 (1970).
5. G. BROSTIGEN AND A. KJEKSHUS, *Acta Chem. Scand.* **24**, 2993 (1970).
6. A. KJEKSHUS AND D. G. NICHOLSON, *Acta Chem. Scand.* **25**, 866 (1971).
7. J. B. GOODENOUGH, Metallic Oxides, in "Progress in Solid State Chem." Vol. 5 (H. Reiss, Ed.), Pergamon, N.Y., 1971.
8. J. B. GOODENOUGH, Colloques Internationaux du CNRS No. 157 (Editions du CNRS, 1967); *J. Phys. Chem. Solids* **30**, 261 (1969).
9. J. B. GOODENOUGH, *J. Solid State Chem.* **3**, 26 (1971).
10. H. HOLSETH AND A. KJEKSHUS, *Acta Chem. Scand.* **22**, 3273, 3284 (1968); **23**, 3043 (1969).
11. H. HOLSETH, A. KJEKSHUS AND A. F. ANDRESEN, *Acta Chem. Scand.* **24**, 3309 (1970).
12. A. FAN AND A. WOLD, companion paper.